Supporting Information

Hierarchical Cu_2S Nanorods with Different Crystal Phases for Asymmetrical Supercapacitors and Visible-Light Photocatalysis

Qun Liu,[a] Xiaodan Hong,[a] Xin Zhang,[a] Xingyan You,[a] Xin Zhao,[a]

Xiangyang Liu,[ab] Meidan Ye*[a]*

[a]*Research Institute for Biomimetics and Soft Matter, Fujian Provincial Key Laboratory for Soft Functional Materials Research, Department of Physics, Xiamen University, Xiamen 361005, China*

[b]*Department of Physics, Faculty of Science, National University of Singapore, Singapore*

** Corresponding author: mdye@xmu.edu.cn, liuxy@xmu.edu.cn*

Keywords: hierarchical structures, Cu_2S nanorods, supercapacitors, visible-light photocatalysis

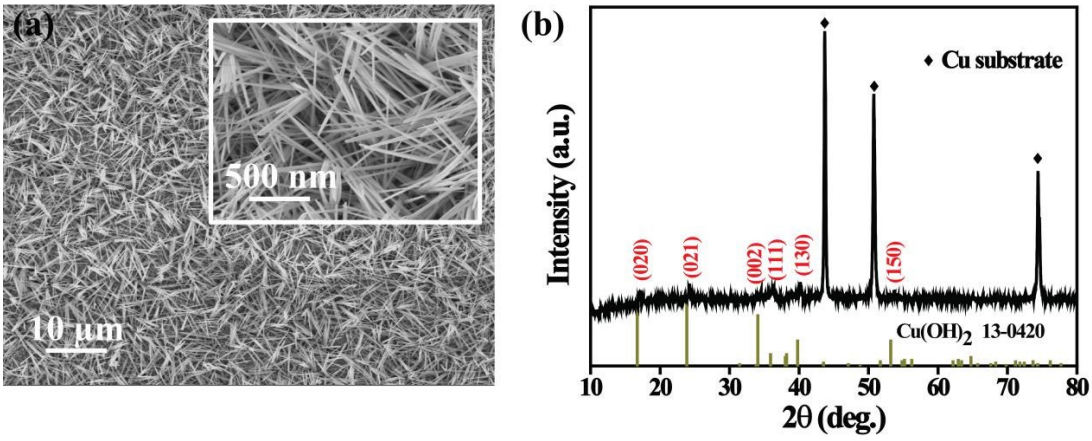

Figure S1. (a) SEM image and (b) XRD pattern of the $Cu(OH)_2$ nanowires.

Table S1. (a)-(c) the EDS for monoclinic and hexagonal nanorods grown on Cu sheets after 6, 12 and 24 hours.

Element / Time	6h	12h	24h
Cu (monoclinic)	61.62	57.62	54.40
S (monoclinic)	34.25	40.34	44.56
Other (monoclinic)	4.13	2.04	1.04
Cu (hexagonal)	59.25	58.26	59.34
S (hexagonal)	30.23	32.56	30.14
Other (hexagonal)	10.52	9.18	10.52

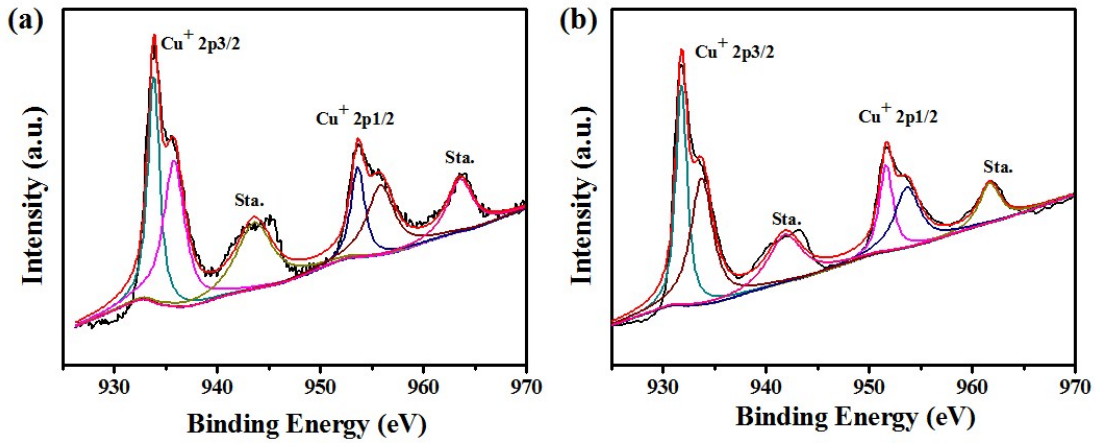

Figure S2. High resolution XPS spectra for the Cu 2p in (a) monoclinic and (b) hexagonal Cu_2S nanorods.

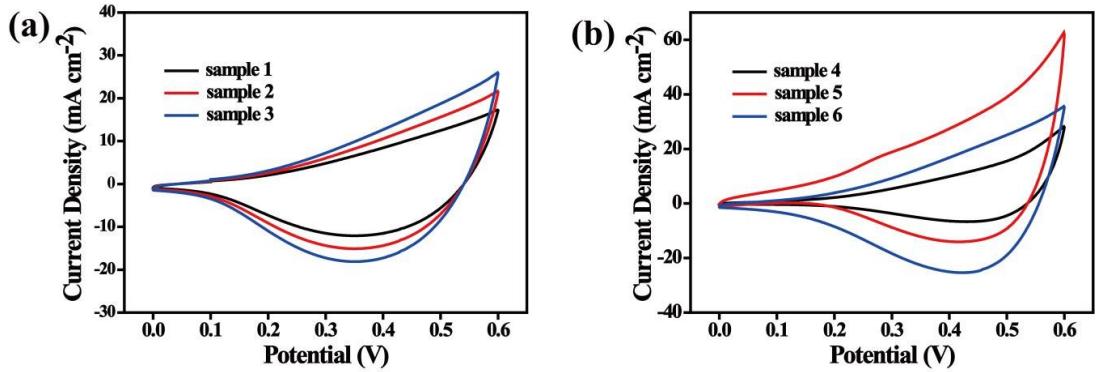

Figure S3. CV curves of the (a) monoclinic and (b) hexagonal Cu_2S nanorods hydrothermally prepared for 6 h, 12 h, and 24 h, respectively.

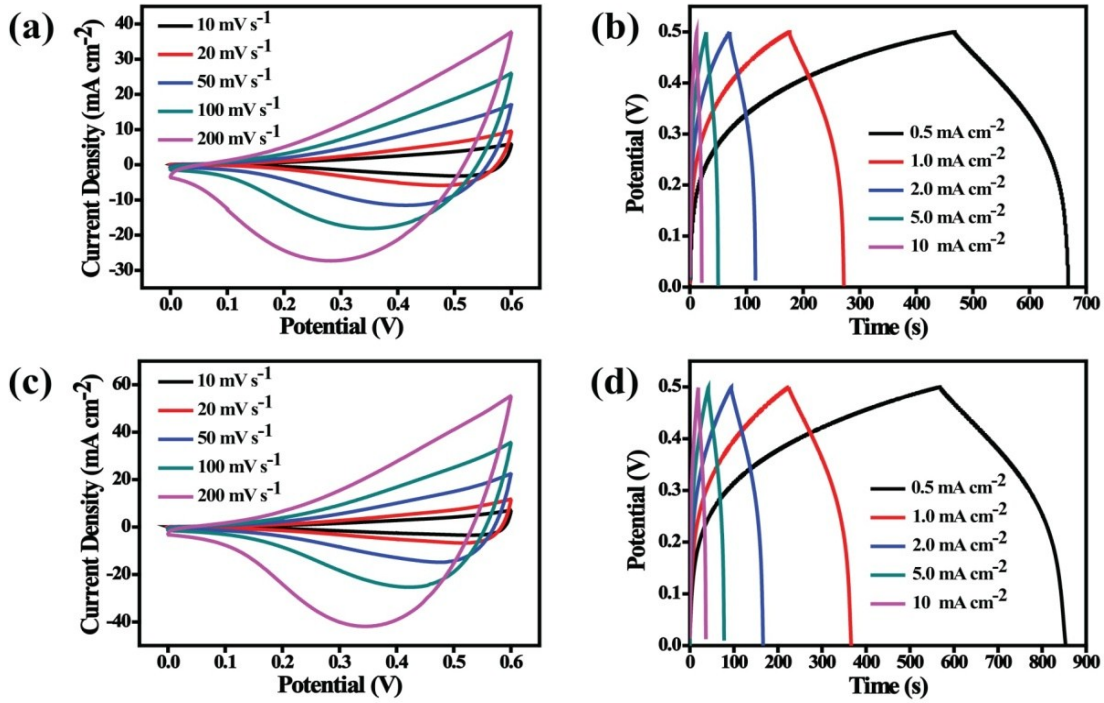

Figure S4. (a) CV curves at different scan rates and (b) GCD curves at various current densities of the monoclinic Cu_2S, (c) CV curves at different scan rates and (d) GCD curves at various current densities of the hexagonal Cu_2S.

Table S2. Comparision of CuX compound.

materials	Specific capacitance (F g^{-1})	Ref.
Cu_2S	375	Present work
CuS	114	1
CuS	305	2
CuO@MnO_2	343.9	3
CuS-SDBS	232.4	4
$Cu(OH)_2$	217 (mF cm^{-2})	5
CuO	346	6

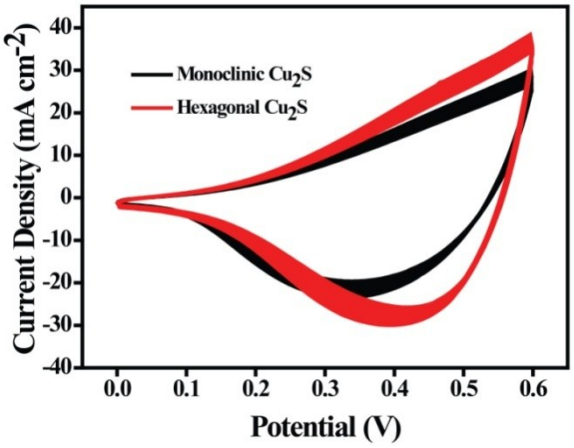

Figure S5. CV curves with 1000 cycles at 100 mV s^{-1} of the monoclinic and hexagonal Cu_2S electrodes.

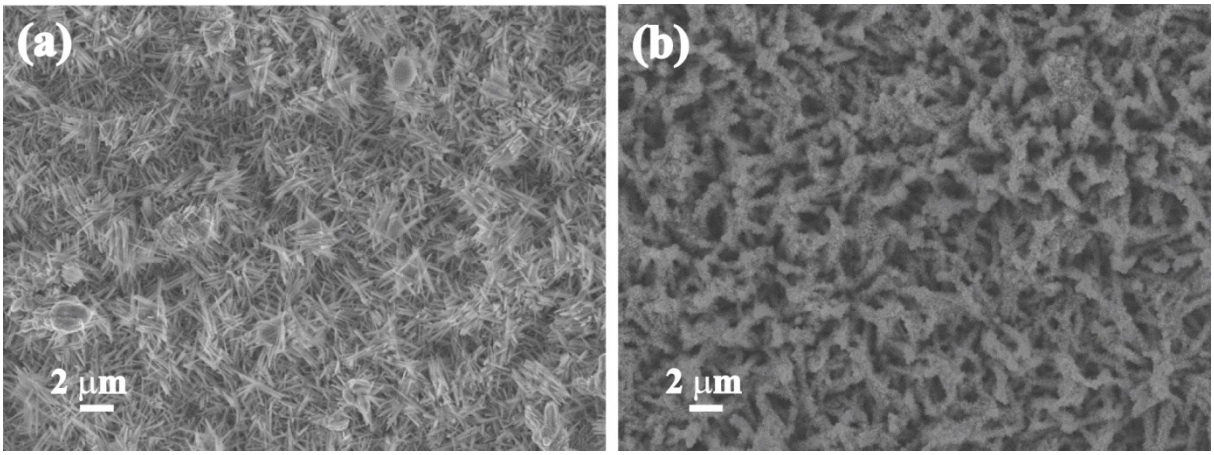

Figure S6. SEM images of the monoclnic and hexagonal Cu_2S films after electrochemical tests for 1000 cycles.

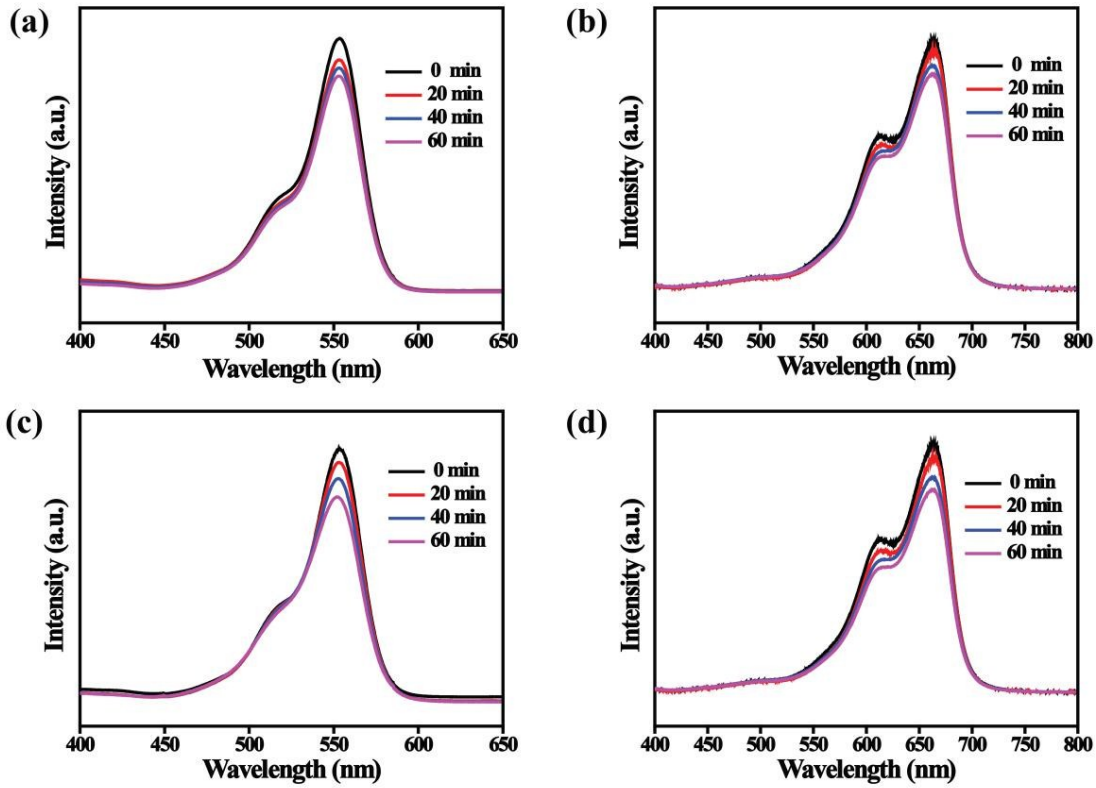

Figure S7. Absorption spectra tracking the photo-degradation of dyes: (a) H_2O_2 + RhB, (b) H_2O_2 + MB, (c) Cu_2S + RhB, (d) Cu_2S + MB.

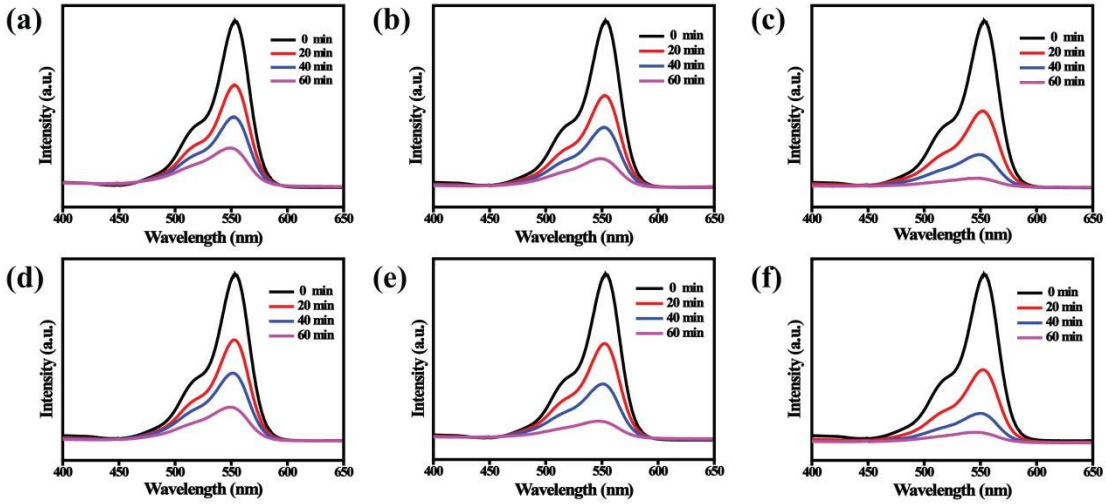

Figure S8. Absorption spectra tracking the photo-degradation of RhB under visible light by different catalysts: the (a-c) monoclinic and (d-f) hexagonal Cu_2S nanorods hydrothermally prepared for 6 h, 12 h, and 24 h, respectively.

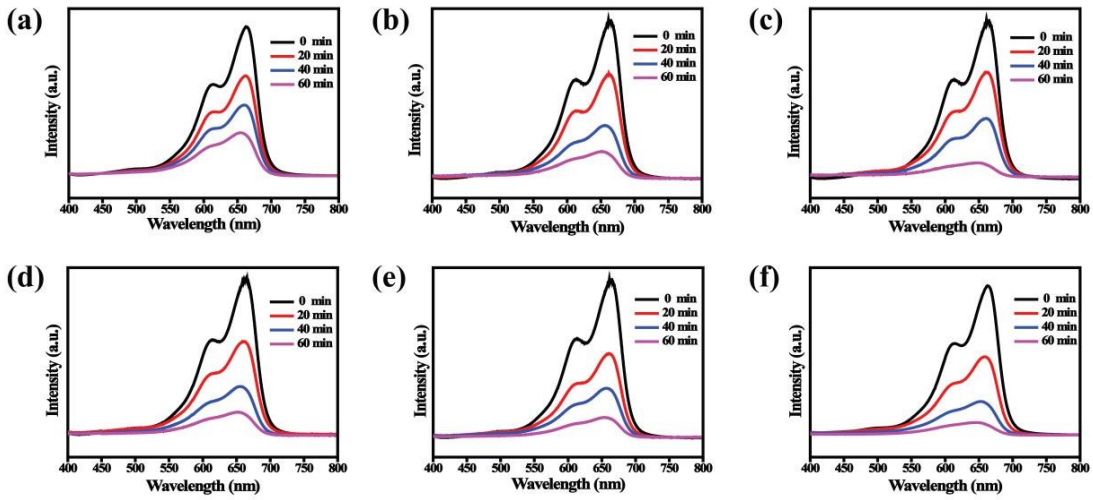

Figure S9. Absorption spectra tracking the photo-degradation of MB under visible light by different catalysts: the (a-c) monoclinic and (d-f) hexagonal Cu_2S nanorods hydrothermally prepared for 6 h, 12 h, and 24 h, respectively.

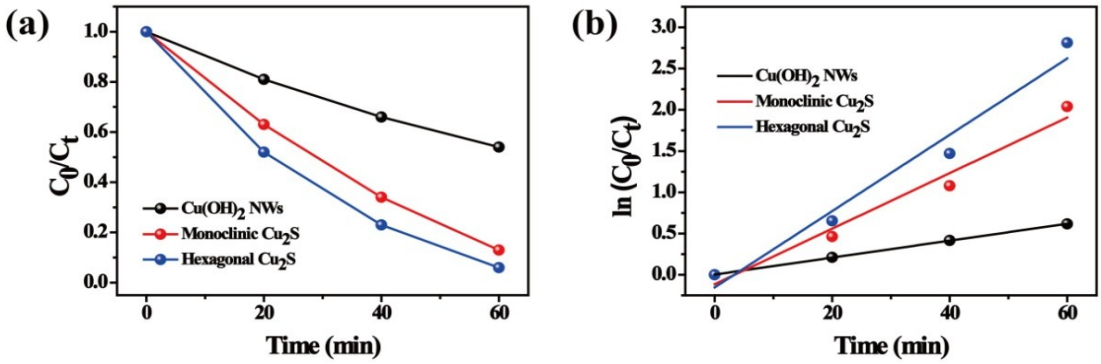

Figure S10. (a) The residual concentration and (b) $\ln(C_0/C_t)$ versus time curves of MB with different catalysts.

Reference

1 T. Zhu, B. Xia, L. Zhou and X. Wen Lou, J. Mater. Chem., 2012, **22**, 7851.

2 Y.-K. Hsu, Y.-C. Chen and Y.-G. Lin, Electrichim. Acta, 2014, **139**, 401-407.

3 H. Chen, M. Zhou, T. Wang, F. Li and Y. X. Zhang, J. Mater. Chem. A, 2016, **4**, 10786-10793.

4 K.-J. Huang, J.-Z. Zhang and Y. Fan, J. Alloy. Compd. 2015, **625**, 158-163.

5 S. Lei, Y. Liu, L. Fei, R. Song, W. Lu, L. Shu, C. L. Mak, Y. Wang and H. Huang, J. Mater. Chem. A, 2016, **4**, 14781-14788.

6. D. P. Dubal, G. S. Gund, R. Holze and C. D. Lokhande, Journal of Power Sources, 2013, **242**, 687-698.